Topic	Source parameters and moment-tensor solutions
Author	**Günter Bock (✞)**, Formerly GeoForschungsZentrum Potsdam, Germany
Version	September 2002; editorially adapted and amended July 2012 (see **Note**); **DOI: 10.2312/GFZ.NMSOP-2_IS_3.8**

Note: Late Dr. G. Bock has been unable to upgrade his former section 3.5 in Chapter 3 of the first NMSOP (2002) edition. It has been reproduced here for the electronic edition of NMSOP-2 with some editorial changes in format and revised web addresses until being complemented by an expanded up-to-date Information Sheet on the topic by Prof. F. Krüger.

Page

1 Introduction

The concept of first order *moment tensor* provides a complete description of equivalent body forces of a general seismic point source (see Figure 1). A source can be considered a point source if both the distance D of the observer from the source and the wavelength λ of the data are much greater than the linear dimension of the source. Thus, moment-tensor solutions are generally derived from low-frequency data and they are representative of the gross properties of the rupture process averaged over tens of seconds or more. The double-couple source model describes the special case of shear dislocation along a planar fault. This model has proven to be very effective in explaining the amplitude and polarity pattern of P, S and surface waves radiated by tectonic earthquakes. In the following, we briefly outline the relevant relations (in a first order approximation) between the moment tensor of a seismic source and the observed seismogram. The latter may be either the complete seismogram, one of its main groups (P, S or surface waves), or specific features of seismograms such as peak-to-peak amplitudes of body waves, amplitude ratios or spectral amplitudes. Then we outline a linear inversion scheme for obtaining the moment tensor using waveform data in the time domain. Finally, we will give an overview of some useful programs for moment-tensor analysis. Applications of moment-tensor inversions to the rapid (i.e., generally within 24 hours after the event) determination of source parameters after significant earthquakes will also be described.

2 Basic relations

Following Jost and Herrmann (1989), the displacement d on the Earth's surface at a station can be expressed, in case of a point source, as a linear combination of time-dependent moment-tensor elements M_{kj} (ξ,t) that are assumed to have the same time dependence convolved (indicated by the star symbol) with the derivative G_{skj} $(\mathbf{x},\xi,t)$ of the Green's functions with regard to the spatial j-coordinate:

$$u_s(\mathbf{x},t) = M_{kj}(\xi,t) * G_{sk,j}(\mathbf{x},\xi,t)\,. \tag{1}$$

$u_s(\mathbf{x}, t)$: s component of ground displacement at position x and time t
$M_{kj}(\xi,t)$: components of 2nd order, symmetrical seismic moment tensor M
$G_{skj}(\mathbf{x},\xi,t)$: derivative of the Green's function with regard to source coordinate ξ_j
$\mathbf{x}$: position vector of station with coordinates x_1, x_2, x_3 for north, east and down
ξ: position vector of point source with coordinates ξ_1, ξ_2, ξ_3 for north, east and down

Eq. (1) follows from the representation theorem in terms of the Green´s function (see Equations (21) and (38) in IS 3.1).The Green's function represents the impulse response of the medium between source and receiver and thus contains the various wave propagation effects through the medium from source to receiver. These include energy losses through reflection and transmission at seismic discontinuities, anelastic absorption and geometrical spreading. The $M_{kj}(\xi,t)$ from Eq.(1) completely describes the forces acting in the source and their time dependence. The Einstein summation notation is applied in Eq. (1) and below, i.e., the repeated indices k and j = 1, 2, 3 imply summation over x_1, x_2 and x_3. In Eq. (1) the higher order terms of the Taylor expansion around the source point of the Green's functions $G_{sk,j}$ $(\mathbf{x},\xi,t)$ have been neglected. Note that the source-time history s(t) (see 3.1, Figs. 3.4 and 3.9), which describes the time dependence of moment released at the source, is contained in c. If we assume that all the components of $M_{kj}(\xi,t)$ have the same time dependence s(t) the equation can be written as:

$$u_s(\mathbf{x}, t) = M_{kj}\ [G_{sk,j}(\mathbf{x},\xi,t) * s(t)] \tag{2}$$

with s(t): source time history.

When determining $M_{kj}(\xi,t)$ from seismic records, $u_s(\mathbf{x}, t)$ is calculated by convolution of the observed seismogram components $y_s(\mathbf{x}, t)$ with the inverse of the seismograph's displacement response function i(t):

$$u_s(\mathbf{x}, t) = y_s(\mathbf{x}, t) * \mathrm{Inv}\{i(t)\}$$

In the frequency domain (see Eq. (14) in IS 3.1) convolution is replaced by multiplication:

$$D_s(\mathbf{x}, \omega) = Y_s(\mathbf{x}, \omega)\, I(\omega)^{-1}$$

where ω is circular frequency. The $D_s(\mathbf{x}, \omega)$, $Y_s(\mathbf{x}, \omega)$, and $I(\omega)^{-1}$ are the respective Fourier transforms of the time series $d_s(\mathbf{x}, t)$, $y_s(\mathbf{x}, t)$, and $i(t)^{-1}$ (see 5.2.7 where $I(\omega)^{-1}$ is denoted as $H_d(\omega)^{-1}$).

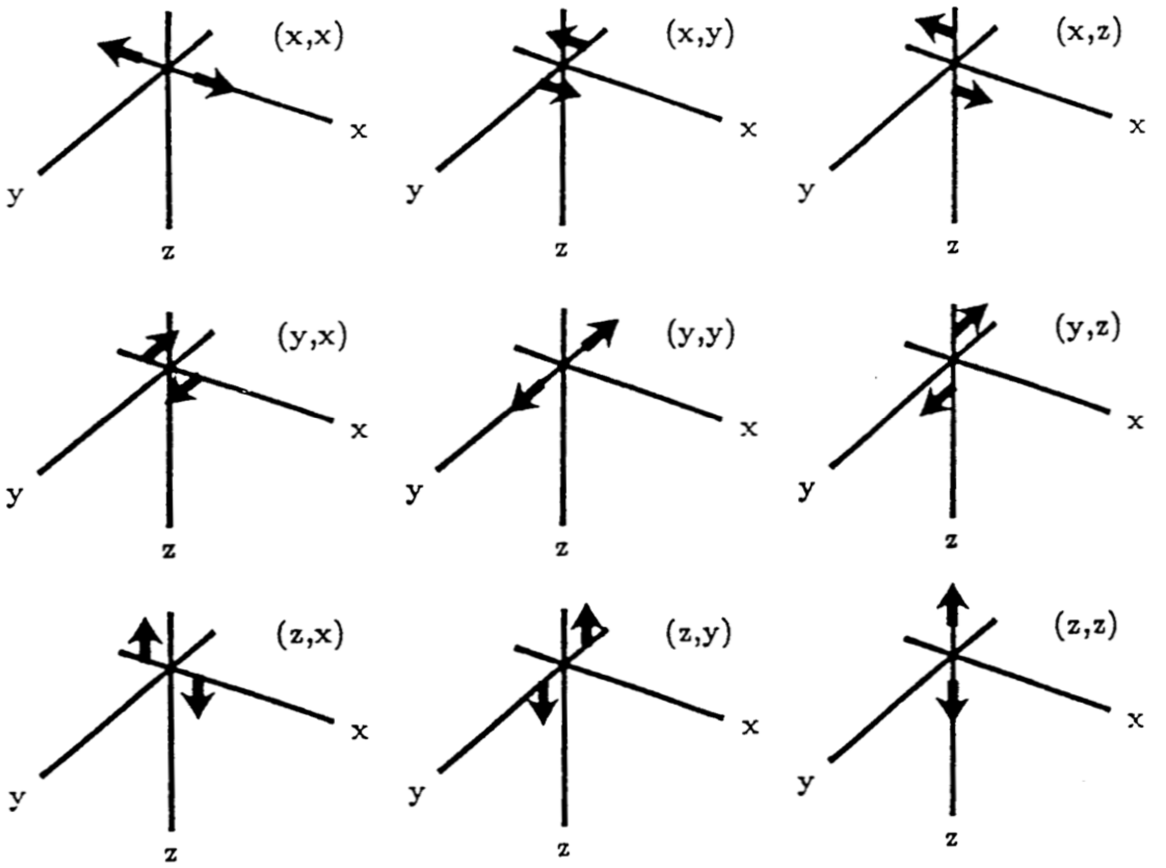

Figure 1 The nine generalized couples representing $G_{sk,j}(\mathbf{x}, \xi, t)$ in Eq. (3.69). Note that force couples acting on the y axis in x direction or vice versa (i.e., (x,y) or (y,x)) will cause shear faulting in the x and y direction, respectively. Superimposition of vector dipoles in x and y direction with opposite sign, e.g., (x,x) + (-y,-y) will also cause shear faulting but 45° off the x and y direction, respectively. Both representations are equivalent (reproduced from Jost and Herrmann, A student's guide to and review of moment tensors. Seismol. Res. Lett., **60**, 2, 1989, Fig. 2, p. 39; ©Seismological Society of America).

In the following we assume that the source-time function s(t) is a delta function (i.e., a "needle" impulse). Then, $M_{kj}(\xi, t) = M_{kj}(\xi)\cdot\delta(t)$, and the right side of Eq.(2) simplifies to $M_{kj}(\xi)\cdot G_{sk,j}(t)$. The seismogram recorded at x can be regarded as product of $G_{sk,j}$ and $M_{kj.}$ (e.g., Aki and Richards, 1980 and 2002; Lay and Wallace, 1995; Udias, 1999). Thus, the derivative of G_{skj} with regard to the source coordinate ξ_i describes the response to a single couple with its lever arm pointing in the ξ_j direction (see Figure 1). For k = j we obtain a vector dipole; these are the couples (x,x), (y,y), and (z,z) in Figure 1. A double-couple source is characterized by a moment tensor where one eigenvalue of the moment tensor vanishes (equivalent to the Null or B axis), and the sum of eigenvalues vanishes, i.e., the trace of the moment tensor is zero. Physically, this is a representation of a shear dislocation source without any volume changes.

Using the notation of Figure 1, double-couple displacement fields are represented by the sum of two couples such as (x,y)+(y,x), (x,x)+(y,y), (y,y)+(z,z), (y,z)+(z,y) etc. An explosion source (corresponding to M_6 in Eq. (8) and Figure 2) can be modelled by the sum of three vector dipoles (x,x) + (y,y) + (z,z). A compensated linear vector dipole (CLVD, see section 4 below) can be represented by a vector dipole of strength 2 and two vector dipoles of unit strength but opposite sign in the two orthogonal directions.

The seismic moment tensor **M** has, in general, six independent components which follows from the condition that the total angular momentum for the equivalent forces in the source must vanish. For vanishing trace, i.e., without volume change, we have five independent components that describe the deviatoric moment tensor. The double-couple source is a special case of the deviatoric moment tensor with the constraint that the determinant of **M** is zero, i.e., that the stress field is two-dimensional.

In general, **M** can be decomposed into an isotropic and a deviatoric part:

$$\mathbf{M} = \mathbf{M}^{\text{isotropic}} + \mathbf{M}^{\text{deviatoric}}. \tag{3}$$

The decomposition of **M** is unique while further decomposition of $\mathbf{M}^{\text{deviatoric}}$ is not. Commonly, $\mathbf{M}^{\text{deviatoric}}$ is decomposed into a double couple and CLVD:

$$\mathbf{M}^{\text{deviatoric}} = \mathbf{M}^{\text{DC}} + \mathbf{M}^{\text{CLVD}}. \tag{4}$$

For a double-couple source, the Cartesian components of the moment tensor can be expressed in terms of strike ϕ, dip δ and rake λ of the shear dislocation source (fault plane), and the scalar seismic moment M_0 (Aki and Richards, 1980):

$$\begin{aligned}
M_{xx} &= -\, M_0(\sin\delta \cos\lambda \sin2\phi \;+\; \sin2\delta \sin\lambda \sin^2\phi)\\
M_{xy} &= \;\; M_0(\sin\delta \cos\lambda \cos2\phi \;+\; 0.5 \sin2\delta \sin\lambda \sin2\phi)\\
M_{xz} &= -\, M_0(\cos\delta \cos\lambda \cos\phi \;+\; \cos2\delta \sin\lambda \sin\phi)\\
M_{yy} &= \;\; M_0(\sin\delta \cos\lambda \sin2\phi \;-\; \sin2\delta \sin\lambda \cos^2\phi)\\
M_{yz} &= -\, M_0(\cos\delta \cos\lambda \sin\phi \;-\; \cos2\delta \sin\lambda \cos\phi)\\
M_{zz} &= \;\; M_0 \sin2\delta \sin\lambda
\end{aligned} \tag{5}$$

As the tensor is always symmetric it can be rotated into a principal axis system such that all non-diagonal elements vanish and only the diagonal elements are non-zero. The diagonal elements are the *eigenvalues* (see Eq. (6) in Information Sheet 3.1) of **M**; the associated directions are the *eigenvectors* (i.e., the *principal axes*). A linear combination of the principal moment-tensor elements completely describes the radiation from a seismic source. In the case of a double-couple source, for example, the diagonal elements of **M** in the principal axis system have two non-zero eigenvalues M_0 and $-M_0$ (with M_0 the scalar seismic moment) whose eigenvectors give the direction at the source of the tensional (positive) T axis and compressional (negative) P axis, respectively, while the zero eigenvalue is in the direction of the B (or Null) axis of the double couple (for definition and determination of M_0 see Exercise 3.4).

Eq. (2) describes the relation between seismic displacement and moment tensor in the time domain. If the source-time function is not known or the assumption of time-independent moment-tensor elements is dropped, e.g., for reasons of source complexity, the frequency-domain approach is chosen:

$$u_s(\mathrm{x}, f) = M_{kj}(f)G_{sk,j}(\mathrm{x}, \xi, f) \tag{6}$$

where f denotes frequency. Procedures for the linear moment-tensor inversion can be designed in both the time and frequency domain using Eq. (2) or (6). We can write (2) or (6) in matrix form:

$$\mathbf{u} = \mathbf{G}\ \overline{m}. \tag{7}$$

In the time domain, the **u** is a vector containing n sampled values of observed ground displacement at various times, stations and sensor components, while **G** is a $6 \times n$ matrix and the vector $\overline{m}$ contains the six independent moment-tensor elements to be determined. In the frequency domain, **u** contains k complex values of the displacement spectra determined for a given frequency f at various stations and sensor components. G is a $6 \times$ k matrix and is generally complex like $\overline{m}$. For more details on the inversion problem in Eq. (7) the reader is referred to Chapter 6 in Lay and Wallace (1995), Chapter 12 in Aki and Richards (1980), or Chapter 19 of Udias (1999).

To invert Eq. (7) for the unknown $\overline{m}$, one has to calculate the derivatives of the Green's functions. The calculation of the Green's functions constitutes the most important part of any moment-tensor inversion scheme. A variety of methods exists to calculate synthetic seismograms (e.g., Müller, 1985; Doornbos, 1988; Kennett, 1988). Some of the synthetic seismogram codes allow calculations for the moment-tensor elements as input source while others allow input for double-couple and explosive point sources. The general moment tensor can be decomposed in various ways using moment-tensor elements of double-couple and explosive sources so that synthetic seismogram codes employing these source parameterizations can also be used in the inversion of (7).

3 An inversion scheme in the time domain

In this section, we will describe in short the moment-tensor inversion algorithm of Kikuchi and Kanamori(1991), where the moment tensor is decomposed into elementary double-couple sources and an explosive source. Adopting the notation used by Kikuchi and Kanamori(1991), the moment tensor M_{kj} is represented by a linear combination of $N_\mathrm{e} = 6$ elementary moment tensors M_n (Figure 2):

$$M_{kj} = \sum_{n=1}^{N_e} a_n M_n \tag{8}$$

with $M_1 : \begin{bmatrix} 0 & 1 & 0 \\ 1 & 0 & 0 \\ 0 & 0 & 0 \end{bmatrix}$; $M_2 : \begin{bmatrix} 1 & 0 & 0 \\ 0 & -1 & 0 \\ 0 & 0 & 0 \end{bmatrix}$; $M_3 : \begin{bmatrix} 0 & 0 & 0 \\ 0 & 0 & 1 \\ 0 & 1 & 0 \end{bmatrix}$

$$M_4: \begin{bmatrix} 0 & 0 & 1 \\ 0 & 0 & 0 \\ 1 & 0 & 0 \end{bmatrix};\ M_5: \begin{bmatrix} -1 & 0 & 0 \\ 1 & 0 & 0 \\ 0 & 0 & 1 \end{bmatrix};\ M_6: \begin{bmatrix} 1 & 0 & 0 \\ 0 & 1 & 0 \\ 0 & 0 & 1 \end{bmatrix}$$

The M_1 and M_2 represent pure strike-slip faults; M_3 and M_4 represent dip-slip faults on vertical planes striking N-S and E-W, respectively, and M_5 represents a 45° dip-slip fault. The M_6 represents an isotropic source radiating energy equally into all directions (i.e., an explosion).

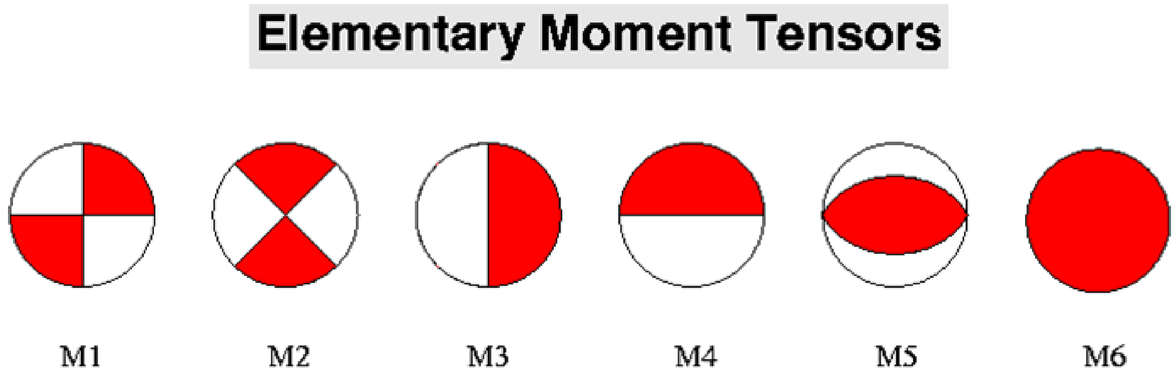

Figure 2 Elementary moment tensors used in the inversion of the full moment tensor (after Kikuchi and Kanamori, 1991)

A pure deviatoric moment tensor (trace(M_{kj}) = 0) is entirely represented by the five elementary moment tensors M_1 to M_5. The following brief description of the linear inversion for the moment tensor (Kikuchi and Kanamori, 1991) is an example of an inversion performed in the time domain. It can be easily adopted for an inversion in the frequency domain by replacing the time series by their spectra. Let $w_{sn}(t)$ denote the Green's function derivative at station s in response to the elementary moment *tensor* M_n, and let $x_S(t)$ be the observed ground displacement as function of time at station *s*. The best estimate for the coefficients a_n in Eq. (8) can be obtained from the condition that the difference between observed and synthetic displacement functions be zero:

$$\begin{aligned} \Delta &= \sum_{s=1}^{N_s} \int \left[x_s(t) - \sum_{n=1}^{N_e} a_n w_{sn}(t) \right]^2 dt \\ &= R_x - 2\sum_{n=1}^{N_e} a_n G_n + \sum_{m=1}^{N_e} \sum_{n=1}^{N_e} R_{nm} a_n a_m \\ &= Minimum \end{aligned} \tag{9}$$

The N_e is the number of elementary moment tensors, and N_s is the number of displacement records used. The other terms in (9) are given by:

$$R_x = \sum_{s=1}^{N_s} \int [x_s(t)]^2\, dt$$

$$R_{nm} = \sum_{s=1}^{N_S} \int [w_{sn}(t) w_{sm}(t)]\, dt$$

$$G_n = \sum_{s=1}^{N_S} \int [w_{sn}(t) x_s(t)]\, dt$$

Integration is carried out over selected portions of the waveforms. Evaluating $\partial\Delta/\partial a_n = 0$ for $n = 1,..., N_e$ yields the normal equations

$$\sum_{m=1}^{N_e} R_{nm} a_m = G_n \tag{10}$$

with n ranging from 1 to N_e. The solution for a_n is given by:

$$a_n = \sum_{m=1}^{N_e} R_{nm}^{-1} G_m \tag{11}$$

The inverse R_{nm}^{-1} of matrix R_{nm} can be obtained by the method of generalized least squares inversion (e.g., Pavlis, 1988). The resultant moment tensor is then given by

$$M_{kj} \begin{bmatrix} a_2 - a_5 + a_6 & a_1 & a_4 \\ a_1 & -a_2 + a_6 & a_3 \\ a_4 & a_3 & a_5 + a_6 \end{bmatrix} \tag{12}$$

The variance of the elements a_n can be calculated under the assumption that the data are statistically independent:

$$\mathrm{var}(a_n) = \sum_{m=1}^{N_e} (R_{nm}^{-1})^2 \sigma_m^2$$

where σ_m^2 is the variance of the data G_n. In the case where the variance of the data is not known, $\sum_{m=1}^{N_e} (R_{nm}^{-1})^2$ can be used as relative measure for the uncertainty.

4 Decomposition of the moment tensor

Except for the volumetric and deviatoric components, the decomposition of the moment tensor is not unique. Useful computer programs for decomposition were written by Jost and distributed in Volume VIII of the Computer Programs in Seismology by Herrmann of Saint Louis University (http://www.eas.slu.edu/People/RBHerrmann/ComputerPrograms.html or e-mail to R. W. Herrmann: rbh@slueas.slu.edu). The first step in the decomposition is the calculation of eigenvalues and eigenvectors of the seismic moment tensor. For this the program *mteig* can be used. It performs rotation of the moment tensor **M** into the principal axis system. The eigenvector of the largest eigenvalue gives the T (or tensional) axis; the eigenvector of the smallest eigenvalue gives the direction of the P (or compressional) axis, while the eigenvector associated with the intermediate eigenvalue gives the direction of the Null axis. The output of *mteig* is the diagonalized moment tensor

$$M = \begin{bmatrix} m_1 & 0 & 0 \\ 0 & m_2 & 0 \\ 0 & 0 & m_3 \end{bmatrix} \tag{13}$$

whose elements are input to another program, *mtdec*, which performs a moment-tensor decomposition. First, the moment tensor is decomposed into an isotropic and a deviatoric part (see Eq. 3):

$$M = \frac{1}{3}\begin{bmatrix} tr(M) & 0 & 0 \\ 0 & tr(M) & 0 \\ 0 & 0 & tr(M) \end{bmatrix} + \begin{bmatrix} m_1^1 & 0 & 0 \\ 0 & m_2^1 & 0 \\ 0 & 0 & m_3^1 \end{bmatrix} \tag{14}$$

with $tr(\mathbf{M}) = m_1 + m_2 + m_3$ being the trace of **M**. The isotropic part of **M** is important in quantifying volume changes of the source, but it is usually difficult to resolve so that isotropic parts of less than 10% are often not considered to be significant. The deviatoric part of the moment tensor can be further decomposed. Options include decompositions into three vector dipoles, into three double couples, into 3 CLVD sources, into a major and minor double couple, and into a best double couple and a CLVD having the same principal axis system. The source mechanisms reported by Harvard and USGS are based on the decomposition of the moment tensor into a best double couple and a CLVD. In addition to the best double couple they also provide the moment-tensor elements. To estimate the double-couple contribution to the deviatoric moment tensor, the parameter

$$\varepsilon = \frac{|m_{\min}|}{|m_{\max}|}$$

is used (Dziewonski et al., 1981) where m_{min} and m_{max} are the smallest and largest eigenvalues of the deviatoric part of **M**, respectively, both in absolute terms. For a pure double-couple source, $\varepsilon = 0$ because $m_{min} = 0$; for a pure CLVD, $\varepsilon = 0.5$. The percentage double-couple contribution can be expressed as $(1-2\varepsilon)\times 100$. Significant CLVD components are often reported for large intermediate-depth and very deep earthquakes. In many cases, however, it can be shown that these are caused by superposition of several rupture events with different double-couple mechanisms (Kuge and Kawakatsu, 1990; Frohlich, 1995; Tibi et al., 1999).

Harvard and USGS publish the moment tensors using the notation of normal mode theory. It is based on spherical co-ordinates $(r;\Theta;\Phi)$ where r is the radial distance of the source from the center of the Earth, Θ is co-latitude, and Φ is longitude of the point source. The 6 independent moment-tensor elements in the (x, y, z) = (north, east, down) coordinate system are related to the components in (r;Θ;Φ) by

$$M_{rr} = M_{zz}$$

$$M_{\Theta\Theta} = M_{xx}$$

$$M_{\Phi\Phi} = M_{yy}$$

$$M_{r\Theta} = M_{zx}$$

$$M_{r\Phi} = -M_{zy}$$

$$M_{\Theta\Phi} = -M_{xy}$$

5 Steps taken in moment-tensor inversion

Generally, the quality of moment-tensor inversion depends to a large extent on the number of data available and the azimuthal distribution of stations about the source. Dufumier (1996) gives a systematic overview for the effects caused by differences in the azimuthal coverage and the effects caused due to the use of only P waves, P plus SH waves or P and SH and SV waves for the inversion with body waves.

A systematic overview with respect to the effects caused by an erroneous velocity model for the Green function calculation and the effects due to wrong hypocenter coordinates can be found in Šílený et al. (1992), Šílený and Pšenčik (1995), Šílený et al. (1996) and Kravanja et al. (1999).

The following is a general outline of the various steps to be taken in a moment-tensor inversion using waveform data:

1) Data acquisition and pre-processing
- good signal-to-noise ratio
- unclipped signals
- good azimuthal coverage
- removing mean value and linear trends
- correcting for instrument response, converting seismograms to displacement
  low-pass filtering to remove high-frequency noise and to satisfy the point source approximation

2) Calculation of synthetic Green's functions dependent on
- Earth model
- location of the source
- receiver position

3) Inversion

- selection of waveforms, e.g., P, S H or full seismograms
- taking care to match waveforms with corresponding synthetics
- evaluation of Eqs. (8) and (9)
- decomposition of moment tensor, e.g., into best double couple plus CLVD

The inversion may be done in the time domain or frequency domain. Care must be taken to match the synthetic and observed seismograms. Alignment of observed and synthetic waveforms is facilitated by cross-correlation techniques. In most moment-tensor inversion schemes, focal depth is assumed to be constant. The inversion is done for a range of focal depths and as best solution one takes that with the minimum variance of the estimate.

6 Some methods of moment-tensor inversion

6.1 NEIC fast moment tensors

This is an effort by the U.S. National Earthquake Information Center (NEIC) in co-operation with the IRIS Data Management Center to produce rapid estimates of the seismic moment tensor for earthquakes with body-wave magnitudes ≥ 5.8. Digital waveform data are quickly retrieved from "open" IRIS stations and transmitted to NEIC by Internet. These data contain teleseismic P waveforms that are used to compute a seismic moment tensor using a technique based on optimal filter design (Sipkin, 1982). Near real-time Current Fast Moment Tensor Solutions are available via http://earthquake.usgs.gov/earthquakes/eqarchives/fm/ . One can also subscribe via https://sslearthquake.usgs.gov/ens/ to a free Earthquake Notification Service (ENS) that sends automated notification E-mails when earthquakes happen in the area of interest to the subscriber

6.2 Harvard and Lamont CMT solutions

The Harvard group developed and maintained an extensive catalog of centroid moment-tensor (CMT) solutions for strong (mainly M > 5.5) earthquakes over the period from 1976-2006. Since then it is maintained and continued by the Global Centroid Moment Tensor Project (GCMT) at the Lamont-Doherty Earth Observatory (LDEO) of Columbia University. The main dissemination point for information and results from this project (e.g., description of the CMT procedure, global CMT Catalog Search, CMT catalog and quick CMT ACII files, special studies of particular earthquakes or sets of earthquakes) is now via the website http://www.globalcmt.org. The Harvard CMT method makes use of both very long-period (T > 40 s) body waves (from the P wave onset until the onset of the fundamental modes) and so-called mantle waves at T > 135 s that comprise the complete surface-wave train. Starting with earthquakes in 2004, the GCMT analysis includes now also intermediate-period surface waves in the moment-tensor inversion. This allows the globally uniform determination of moment tensors for earthquakes down to Mw = 5.0 (Ekström et al., 2012).

Besides the moment tensor the iterative inversion procedure seeks a solution for the best point source location of the earthquake. This is the point where the system of couples is located in the source model described by the moment tensor. It represents the integral of the moment density over the extended rupture area. This centroid location may, for very large earthquakes, significantly differ from the hypocenter location based on arrival times of the first P-wave onsets. The hypocenter location corresponds to the place where rupture started. Therefore, the offset of the centroid location relative to the hypocentral location gives a first indication on fault extent and rupture directivity. In case of the August 17, 1999 Izmit (Turkey) earthquake the centroid was located about 50 km east of the "P-wave" hypocenter. The centroid location coincided with the area where the maximum surface ruptures were observed.

6.3 EMSC and GFZ rapid source parameter determinations

This is an initiative of the European-Mediterranean Seismological Center (Bruyeres-le-Chatel, France, http://www.emsc-csem.org/) and the GEOFON Programs at the GeoForschungs-Zentrum Potsdam (http://www.gfz-potsdam.de/geofon/). The EMSC method uses a grid search algorithm to derive the fault-plane solutions and seismic moments of earthquakes (M > 5.5) in the European-Mediterranean area. Solutions are derived within 24 hours after the occurrence of the event. The data used are P- and S-wave amplitudes and polarities. Figure 3 shows one of the early examples of the kind of output data produced. Nowadays near real-time CMT solutions also for earthquakes world-wide can be obtained via http://geofon.gfz-potsdam.de/eqinfo/ and one may also **subscribe** receiving automatic earthquake notification e-mails by filling-in the Alert Mailing List Registration form of the GEOFON Rapid Earthquake Information Service (see link via http://www.gfz-potsdam.de/geofon/).

6.4 Relative moment-tensor inversion

Especially for the inversion of local events so called relative moment-tensor inversion schemes have been developed (Oncescu, 1986; Dahm, 1996). If the sources are separated by not more than a wavelength, the Green's functions can be assumed to be equal with negligible error. In this case it is easy to construct a linear equation system that relates the moment-tensor components of a reference event to those of another nearby event. This avoids the calculation of high-frequency Green's functions necessary for small local events and all problems connected with that (especially the necessity of modeling site transfer functions in detail).

This is a very useful scheme for the analysis of aftershocks if a well determined moment tensor of the main shock is known. Moreover, if enough events with at least slightly different mechanisms and enough recordings are available, it is also possible to eliminate the reference mechanism from the equations (Dahm, 1996). This is interesting for volcanic areas where events are swarm-like and of similar magnitude, and where a reference moment tensor can not be provided (Dahm and Brandsdottir, 1997).

6.5 NEIC broadband depths and fault-plane solutions

Moment-tensor solutions, which are generally derived from low-frequency data, reflect the gross properties of the rupture process averaged over tens of seconds or more. These solutions may differ from solutions derived from high frequency data, which are more sensitive to the dynamic part of the rupture process during which most of the seismic energy is radiated. For this reason, beginning January 1996, the NEIC has determined, whenever possible, a fault plane solution and depth from broadband body waves for any earthquake having a magnitude greater than about 5.8 and it has published the source parameters in the Monthly Listings of the PDE. The broadband waveforms that are used have a flat displacement response over the frequency range 0.01-5.0 Hz. (This bandwidth, incidentally, is also commensurate with that used by the NEIC to compute teleseismic E_S.) Initial constraints on focal mechanism are provided by polarities from P, pP and PKP waves, as well as by Hilbert-transformed body waves of certain secondary arrivals (e.g., PP), and from transversely polarized S waves. The fault-plane solution and depth are then refined by least-squares fitting of synthetic waveforms to teleseismically recorded P-wave groups (consisting of direct P, pP and sP). More information can be found under http://neic.usgs.gov/neis/nrg/bb_processing.html.

European-Mediterranean Seismological Centre
Centre Sismologique Euro-Mediterraneen

Double-couple solution provided by GFZ Potsdam

EMSC event parameters: 21-JUN-2000_00:51:46.6
63.88 N 20.69 W (Iceland)
Depth = 10 km (adopted in inversion)
Depth = 9 km (based on 32 depth phases)

32 stations used in inversion:

Station	Delta	Azimuth	Takeoff	Polarity
adk	63.06	343.55	20.3	C
aqu	29.12	121.60	27.6	C
biny	38.06	262.06	26.1	x
brg	22.41	109.49	33.8	C
cart	28.87	146.49	27.7	C
cmb	60.57	296.59	20.9	C
cmla	26.31	188.62	28.2	D
cor	56.07	302.72	22.0	C
css	43.52	105.32	24.9	C
dug	55.68	291.95	22.1	C
eil	48.77	107.33	23.7	C
ffc	39.71	296.00	25.8	C
furi	68.86	114.32	19.0	C
hgn	19.27	120.81	34.9	C
incn	75.70	26.33	17.4	D
kev	19.21	51.83	34.9	D
kmbo	77.57	119.84	17.0	C
kbs	17.85	20.07	40.1	D
kwp	27.08	101.36	28.0	C
morc	24.75	106.92	28.4	C
mrni	46.08	104.64	24.3	C
mte	24.76	155.63	28.4	C
pas	63.05	292.64	20.3	C
pet	58.94	331.77	21.3	C
rgn	19.51	103.10	34.8	C
selv	28.58	151.01	27.7	C
sfuc	28.62	155.24	27.7	C
sjg	55.09	235.67	22.2	D
sspa	40.16	262.47	25.7	D
suw	24.19	93.73	28.5	C
tns	20.68	118.00	34.5	C
tuc	61.55	285.54	20.7	C

Data provided by:
IRIS/USGS, MedNet, USNSN, GRSN, UCM/SFO/GEOFON, IRIS/IDA, GEOFON, GII/GEOFON, KNMI, IRIS/GEOFON, IRIS/AWI/GEOFON, TERASCOPE, GRSN/GEOFON, IAG, GTSN, U. Arizona

Corner frequencies of bandpass filter: 0.020 and 0.100 Hz

First fault plane: Strike = 358 degrees
Rake = 185 degrees
Dip = 85 degrees

Second fault plane: Strike = 268 degrees
Rake = -5 degrees
Dip = 85 degrees

M_0 = (4.3 +/- 2.1)*10**18 N*m
Mw = 6.4

Source duration = 4 s (from BB displacement seismograms)

Principal axes	Trend	Plunge
P	223	7
N	43	83
T	313	0

```
                N
                |
        ########---------
       ##########----------
     T ##########------------
   #   ##########-------------
  ###############--------------
 ################---------------
 ################---------------
#################----------------
#############----###############-
------------------###############
------------------###############
 ---------- -------##############
 -----------------##############
  ---   ----------#############
   -- P ----------############
    -   ----------###########
      -----------##########
        ---------########
                |
                S
```

Done by G. Bock, GeoForschungsZentrum Potsdam.
Visit the GFZ-EMSC web page under http://www.gfz-potsdam.de/pb2/pb24/emsc/emsc.html

Figure 3 Example of output data produced by the routine procedure for rapid EMSC source parameter determinations by the GEOFON group at the GFZ Potsdam.

Acknowledgments

The author acknowledges with thanks helpful reviews by A. Udias and W. Brüstle.

Recommended overview readings

Aki and Richards (1980 and 2002)
Ben Menahem and Singh (2000)
Das and Kostrov (1988)
Lay and Wallace (1995)
Udias (1999)

References

Aki, K., and Richards, P. G. (1980). Quantitative seismology. *Freeman*, San Francisco, Vol. I and II, 932 pp.

Aki, K., and Richards, P. G. (2002). Quantitative seismology. Second Edition, ISBN 0-935702-96-2, *University Science Books*, Sausalito, CA.,xvii + 700 pp.

Ben-Menahem, A. and S.J. Singh (2000). *Seismic Waves and Sources*. 2nd edition, Dover Publications, New York.

Dahm, T. (1996). Relative moment tensor inversion based on ray theory: theory and synthetic tests. *Geophys. J. Int*., **124**, 245-257.

Dahm, T., and Brandsdottir, B. (1997). Moment tensors of micro-earthquakes from the Eyjafjallojokull volcano in South Iceland, *Geophys. J. Int*., **130**, 183-192.

Das, S., and Kostrov, B. V. (1988). Principles of earthquake source mechanics. *Cambridge University Press.*

Doornbos, D. J. (Ed.) (1988a). Seismological algorithms, Computational methods and computer programs. *Academic Press*, New York, xvii + 469 pp.

Dufumier, H. (1996). On the limits of linear moment tensor inversion of teleseismic body wave spectra. *Pageoph*, **147**, 467-482.

Dziewonski, A. M., Chou, T.-A., and. Woodhouse, J. H. (1981). Determination of earthquake source parameters from waveform data for studies of global and regional seismicity. *J. Geophys. Res*., **86**, 2825-2852.

Ekström. G., Nettles, M., and Dziewonski, A. M. (2012). The global CMT project 2004-2010: Centroid-momnetn tensors for 13,017 earthquakes. *Phys. Earth Planet Int*., **200-201**, 1-9.

Frohlich, C. (1995). Characteristics of well-determined non-double-couple earthquakes in the Harvard CMT catalog. Phys. *Earth Planet. Inter*., **91**, 213-228.

Kennett, B. L. N. (1988). Systematic approximations to the seismic wavefields, In: Doornbos (1988a), 237-259.

Kikuchi, M., and Kanamori, H. (1991). Inversion of complex body waves – III. *Bull. Seism. Soc. Am*., **81**, 2335-2350.

Kravanja, S., Panza, G. F., and Šilený, J. (1999). Robust retrieval of a seismic point-source function. *Geophys. J. Int*., **136**, 385-394.

Kuge, K., and Kawakatsu, H. (1990). Analysis of a deep “non double couple” earthquake using very broadband data, *Geophys. Res. Lett.*, **17**, 227-230.

Lay, T., and Wallace, T. C. (1995). *Modern global seismology*. ISBN 0-12-732870-X, Academic Press, 521 pp.

Müller, G. (1985). The reflectivity method: A tutorial. *J. Geophys.*, **58**, 153-174.

Oncescu, M. C. (1986). Relative seismic moment tensor determination for Vrancea intermediate depth earthquakes, *Pageoph*, **124**, 931-940.

Šilený, J., Panza, G. F., and Campus, P. (1992). Waveform inversion for point source moment retrieval with variable hypocentral depth and structural model. *Geophys. J. Int.*, **109**, 259-274.

Šilený, J., and Pšenčik, I. (1995). Mechanisms of local earthquakes in 3-D inhomogeneous media determined by waveform inversion. *Geophys. J. Int.*, **121**, 459-474.

Šilený, J., Campus, P., and Panza, G. F. (1996). Seismic moment tensor resolution by waveform inversion of a few local noisy records - I. Synthetic tests. *Geophys. J. Int.*, **126**, 605-619.

Sipkin, S. A. (1982). Estimation of earthquake source parameters by the inversion of waveform data: synthetic waveforms. *Phys. Earth Planet. Inter.,* **30**, 242-259.

Tibi, R., Bock, G., Xia, Y., Baumbach, M., Grosser, H., Milkereit, C., Karakisa, S., Zünbül, S., Kind, R., and Zschau, J. (2001). Rupture processes of the 1999 August 17 Izmit, and November 12 Düzce (Turkey) earthquakes. *Geophys. J. Int.*, **144,** F1-F7.

Udías, A. (1999). Principles of Seismology. *Cambridge University Press*, United Kingdom, 475 pp.